COMPUTATION OF BEAM COUPLING IMPEDANCE IN THE FREQUENCY DOMAIN BY MEANS OF FIT AND FEM

U. Niedermayer*, O. Boine-Frankenheim, and H. De Gersem
Technische Universität Darmstadt, Institut für Theorie Elektromagnetischer Felder (TEMF), Schlossgartenstraße 8, 64289 Darmstadt, Germany

Abstract

A detailed knowledge of transverse and longitudinal beam coupling impedance is required to quantify intensity thresholds due to coherent instabilities and beam induced heating in ion synchrotrons. Particularly at low frequencies, where the beam pipe dominates the impedance spectrum, analytical calculations are widely used since contemporary time domain methods are inapplicable. We present two different ways to compute beam coupling impedance in the frequency domain. One is based on the Finite Integration Technique (FIT) and it is implemented in 2D and 3D. The staircase FIT approximates curved structures only poorly, therefore another solver is implemented in 2D based on the Finite Element Method (FEM). The unstructured triangular FEM mesh allows to approximate curved structures better. Moreover, it allows to compute the space charge impedance, since the shape of the beam and the beam's dipole moment can be represented properly, such that the direct space charge force can be subtracted and only the coherent force remains. Space charge and resistive wall impedance results for GSI and the upcoming FAIR project and the impedance of the beam pipe for the Future Circular Collider (FCC-hh) design study are presented as applications.

INTRODUCTION

The beam in a synchrotron is modeled as a disc with radius a and surface charge density σ traveling with velocity βc. The displacement d_x of the beam (i.e. a coherent dipole oscillation) can be approximated to first order by

$$\sigma(\varrho, \varphi) \approx \frac{q}{\pi a^2}(\Theta(a-\varrho) + \delta(a-\varrho) d_\mathrm{x} \cos\varphi). \quad (1)$$

The force acting back on the beam is described by the coupling impedance [1]

$$\underline{Z}_{\parallel}(\omega) = -\frac{1}{q^2}\int_{\mathrm{beam}} \vec{\underline{E}} \cdot \vec{\underline{J}}_{\parallel}^{*} \mathrm{d}V \quad (2)$$

$$\underline{Z}_{\perp,\mathrm{x}}(\omega) = -\frac{\beta c}{(q d_\mathrm{x})^2 \omega}\int_{\mathrm{beam}} \vec{\underline{E}} \cdot \vec{\underline{J}}_{d_\mathrm{x}}^{*} \mathrm{d}V. \quad (3)$$

where the beam current in frequency domain (FD) is obtained from Eq. (1) as

$$\underline{J}_{\mathrm{s,z}}(\varrho, \varphi, z; \omega) = \underline{J}_{\parallel} + \underline{J}_{d_\mathrm{x}} = (\sigma_{\parallel} + \sigma_{d_\mathrm{x}}) e^{-i\omega z/\beta c} \quad (4)$$

such that its magnitude is independent of the beam velocity. Equations (2), (3) can be interpreted as functionals of the solution of Maxwell's equations recast in the curl-curl equation

$$\nabla \times \underline{\nu} \nabla \times \vec{\underline{E}} - \omega^2 \underline{\varepsilon}\, \vec{\underline{E}} = -i\omega \vec{\underline{J}}_\mathrm{s}, \quad (5)$$

with the complex reluctivity $\underline{\nu} = \underline{\mu}^{-1} = (\mu' + i\mu'')/|\underline{\mu}|^2$, and the complex permittivity $\underline{\varepsilon} = \varepsilon_0 \varepsilon_r - i\kappa/\omega$ (conductivity κ) as functions of position and frequency.

FINITE INTEGRATION TECHNIQUE

The FIT discretizes Eq. (5) as

$$\widetilde{\mathbf{C}} \mathbf{M}_{\underline{\nu}} \mathbf{C} \underline{\widehat{\mathbf{e}}} - \omega^2 \mathbf{M}_{\underline{\varepsilon}} \underline{\widehat{\mathbf{e}}} = -i\omega \underline{\widehat{\widehat{\mathbf{j}}}}_\mathrm{s}, \quad (6)$$

usually on a rectangular (staircase) mesh of size $n_p = N_x N_y N_z$. This represents a complex (non-Hermitean) ill conditioned system of size $3n_p \times 3n_p$. A simple way to include the beam entry and exit is to use a Floquet boundary condition, i.e. the longitudinal partial derivative matrix of size $n_p \times n_p$ becomes

$$[\mathbf{P}_z]_{m,n} = \begin{cases} -1, & \text{if} \quad m = n \\ 1, & \text{if} \quad m = n - N_x N_y \\ e^{-i\omega L/v}, & \text{if} \quad m = n - N_x N_y + n_p \\ 0, & \text{else.} \end{cases} \quad (7)$$

Note that $\widetilde{\mathbf{P}} = -\mathbf{P}^\mathrm{H}$ and thus $\widetilde{\mathbf{C}} = \mathbf{C}^\mathrm{H}$, but in the presence of losses Eq. (6) remains non-Hermitean. In the case of only one cell in longitudinal direction one obtaines a 2D scheme, i.e. $\mathbf{P}_z = -1 + \exp(-i\omega\Delta z/v)$ becomes a scalar. Due to the numerical simplicity, it is advantageous to treat distributed impedances of long (2D) structures by means of direct solvers (see [2] and references therein for details). However, as visible in Fig. 1, the dipole source to compute

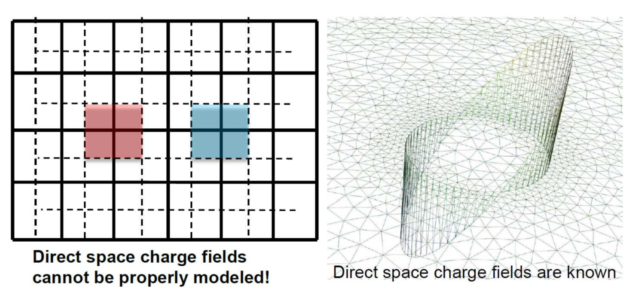

Figure 1: Modeling of the dipole source in the FIT (left) and FEM (right) approach.

the transverse impedance cannot be modeled accurately by the staircase FIT. Thus the direct space charge fields, which depend on the shape of the dipole cannot be removed. This issue is solved by using an unstructured mesh and the finite element method.

* niedermayer@temf.tu-darmstadt.de

ISBN 978-3-95450-136-6

FINITE ELEMENT METHOD

In 2D, Eq. (5) can be solved by the FEM using nodal functions for the longitudinal and Nédélec edge functions [3] for the transverse components (see [4] for details). The implementation is done in Python using the FEniCS package [5, 6]. The mesh originates from Gmsh [7]. Edge functions are advantageous because the tangential electric field on a material boundary is continuous, while the normal one is allowed to have a jump (as is physically correct). Since lowest order edge functions are incapable to representing functions with nonzero divergence, a Helmholtz split has to be applied to Eq. (5). Apart from the additional Poisson system, the curlcurl system presents for lowest order elements an (ill conditioned) complex system of size $n_n + n_e$, which is solved by a direct solver from PETSc, see [8]. The hereby presented code ('BeamImpedance2D', see also [4]) includes also a surface impedance boundary condition (SIBC) $\vec{n}\times\vec{n}\times\underline{\vec{E}} = \underline{Z}_s\vec{n}\times\underline{\vec{H}}$. This allows to simulate the impedance of resistive beam pipes at high frequency without resolving the extremely small skin depth δ in the mesh.

AN APPLICATION FOR FAIR

The extraction kickers for the SIS100 synchrotron consist of a 80 cm long ferrite (Ferroxcube 8C11 [9]) yoke with about 10 cm aperture and 6 cm thickness. The beam scenario with highest intensity and shortest bunch length (single 2E13 protons bunch, $\sigma_s = 3.7$ m) causes the highest stationary heat power as

$$P = \omega_0 \frac{q^2 v^2}{2\pi^2} \int_0^\infty \mathrm{Re}\{\underline{Z}_\parallel(\omega)\}|\underline{\lambda}(\omega)|^2 \mathrm{d}\omega. \quad (8)$$

The impedance of such a kicker device can be strongly reduced by interrupting the magnetic circuit by means of copper sheets in the magnet gap(s). Computation results indicate that for 2.8 mm magnet gaps the heat load is 7327 W with open gaps and 48 W with the gaps filled by a copper sheet (see [10] for more details). As visible in Fig. 2, the FIT and FEM codes obtain roughly the same impedance results. However, note that for curved structures, the staircase FIT code supposedly gives inaccurate results.

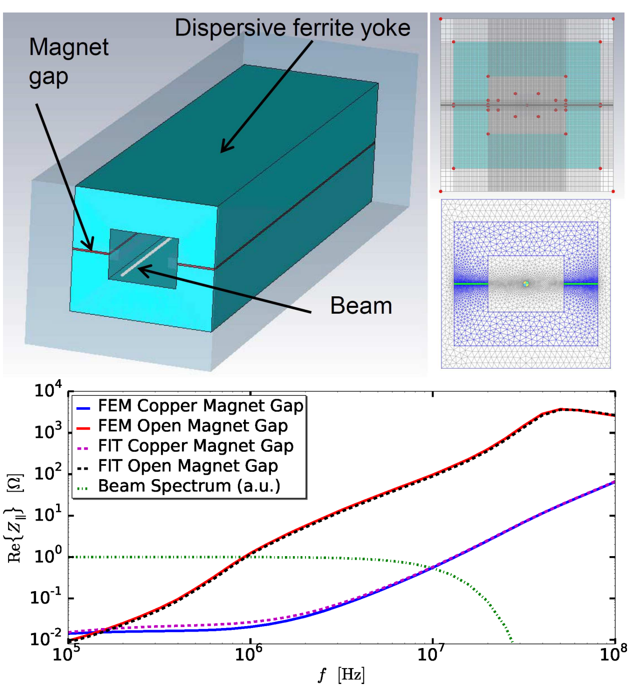

Figure 2: SIS100 transfer kicker magnet, FIT and FEM meshes, and longitudinal impedance results.

AN APPLICATION FOR THE FCC-HH DESIGN STUDY

The future circular collider (FCC) design study aims for a post-LHC accelerator. The hadron-hadron (hh) scenario is outlined for proton collisions up to 100 TeV c.o.m. and a circumference of roughly 100 km [11]. It will be the first hadron accelerator project where synchrotron radiation plays a significant role. Therefore, the beam pipe is designed with a slit and a reflector (see Fig. 3), in order to lead the synchrotron radiation away from the beam (otherwise photo-electrons could build up an unstable electron cloud). Moreover, an impedance reduction is obtained by adding a copper layer of 80μm to the inner surface of the Titanium beam screen.

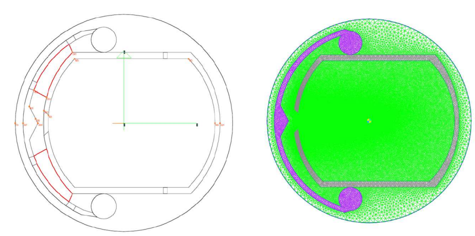

Figure 3: Technical drawing (R. Kersevan, CERN) and Gmsh mesh of the proposed FCC-hh beam pipe.

The transverse impedance of such a complicated structure is computed with BeamImpedance2D. Since only highly conducting materials at low temperature ($RRR \approx 100$) are involved, the SIBC is valid for frequencies down to 100 Hz. However, in order to model the thin copper layer on the titanium pipe, a two-layer SIBC, i.e.

$$\underline{Z}_s(\omega) = \left.\frac{\underline{E}_x}{\underline{H}_y}\right|_{z=0} = \frac{1+i}{\kappa_1\delta_1}\frac{Me^{ik_{z1}d} + Ne^{-ik_{z1}d}}{Me^{ik_{z1}d} - Ne^{-ik_{z1}d}} \quad (9)$$

$$M = 1 + \sqrt{\frac{\mu_1\kappa_2}{\mu_2\kappa_1}}, \quad N = 1 - \sqrt{\frac{\mu_1\kappa_2}{\mu_2\kappa_1}} \quad (10)$$

$$\delta_p = \sqrt{\frac{2}{\mu_p\kappa_p\omega}}, \quad k_{z\,p} = \frac{1-i}{\delta_p}, \quad p = 1, 2 \quad (11)$$

which is the analytic solution of a 1D diffusion problem, is required. A plot of the surface impedance for the cold titanium pipe with copper coating can be seen in Fig. 4.

ISBN 978-3-95450-136-6

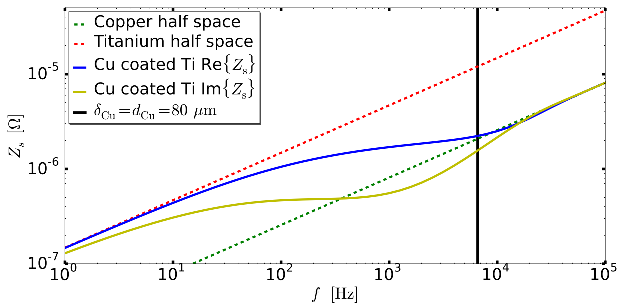

Figure 4: Surface impedance for Copper (κ = 6E7 S/m) coated Titanium (κ = 1.8E6 S/m) with both RRR = 100.

Figure 5 shows the transverse impedance of the pipe, where only the inner vacuum part was meshed and the two-layer SIBC was employed. The results are compared to analytic ones by the Mathematica [12] code Rewall [13] for a round multilayer pipe. As expected, the thick wall impedance lies between the one for minimal and maximal pipe radius. Moreover, the vertical impedance must be larger than the horizontal one, since the vertical aperture is smaller (for a round pipe the transverse impedance scales as $\propto b^{-3}$). The bump of the imaginary part at high frequency is artificial and originates from improper cancellation of space charge impedance at very high γ = 50000, i.e. the error of the space charge impedance is larger than the imaginary part of the resistive wall impedance.

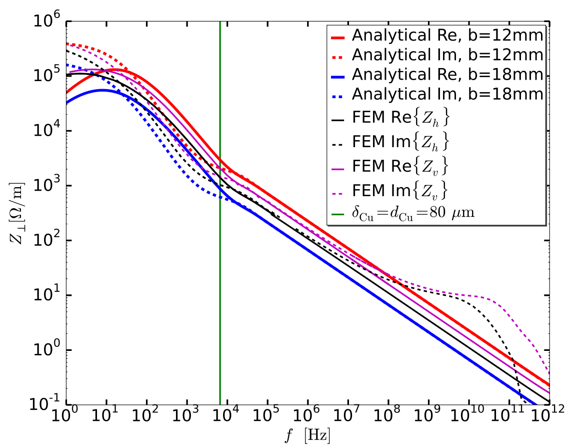

Figure 5: Transverse impedance result for the pipe in Fig. 3 (1 m length) relevant for the Coupled Bunch (at low frequencies) and TMCI (broadband at high frequency) instabilities.

CONCLUSION AND OUTLOOK

Two beam coupling impedance solvers were presented. One is based on FIT and implemented in 2D and 3D using a Floquet boundary condition. The staircase FIT is, however, inappropriate to model curved structures. This is particularly a problem for the transverse impedance at $\beta < 1$, since the direct space charge impedance which outshines the overall imaginary impedance result, is not known for a twin-pencil-beam excitation (Fig. 1) and can thus not be removed. When using an unstructured mesh and the FEM, the source for the dipolar transverse impedance can be modeled as a dipole ring, which has analytically known fields inside. These contributions can be removed up to the accuracy of the field computation. The transverse wall impedance can thus be computed for arbitrary beam velocity. Moreover, the SIBC avoids meshing the wall, which makes this approach applicable up to very high frequencies.

The development of a 3D FEM solver is outlined for the future. Since the Floquet boundary conditions cannot be applied on an unstructured mesh so easy, special beam port boundary conditions will be implemented (see e.g. [14]). The Floquet boundary conditions with FIT, however, can also be employed to compute the impedance of periodic structures. Examples of such are dielectric gratings, which are used in Dielectric Laser Acceleration (DLA), see [15].

ACKNOWLEDGMENT

The authors wish to thank Thilo Egenolf and Fedor Petrov (TEMF) and Xavier Buffat and Daniel Schulte (CERN) for input on the FCC-hh pipe design and Udo Blell (GSI) for input on the SIS100 kicker design.

REFERENCES

[1] R. Gluckstern, CERN Accelerator School (2000).

[2] U. Niedermayer and O. Boine-Frankenheim, Proc. of ICAP'12 (2012).

[3] J.C. Nedelec, Numer. Math. 35, 315-341 (1980).

[4] U. Niedermayer et al., Phys. Rev. –STAB 18, 032001 (2015).

[5] A. Logg, K.-A. Mardal, G.N. Wells, et al., Automated Solution of Differential Equations by the Finite Element Method, Springer (2012).

[6] `www.fenicsproject.org`

[7] C. Geuzaine and J.-F. Remacle, GMSH 2.8.4, `www.geuz.org/gmsh` (2014).

[8] Portable, Extensible Toolkit for Scientific Computation, `http://www.mcs.anl.gov/petsc/`.

[9] Ferroxcube 8C11 Material specification (2002).

[10] U. Niedermayer and O. Boine-Frankenheim, GSI Scientific Report (2013).

[11] `http://www.fcc.web.cern.ch`

[12] Wolfram *Mathematica 9.0®*,`www.wolfram.com` (2013).

[13] N. Mounet and E. Metral, CERN-BE-2009-039, see also `www.cern.ch/imp`

[14] M. Balk, PhD thesis at TU-Darmstadt, Cuvillier Verlag (2005).

[15] J. England et al., Review of Modern Physics (2014).

ISBN 978-3-95450-136-6